

Lightweight Hydraulic Leg to Explore Agile Legged Locomotion

Sang-Ho Hyon, Tomoo Yoneda, Daisuke Suewaka

Abstract—The paper reports on a hydraulic robotic leg, a research platform suitable for exploring high-performance legged locomotion. We propose to use hydraulic linear actuators combined with lightweight links made out from carbon-fiber-reinforced plastic so that we can maximally enjoy their innate high load-to-weight ratio. The robot is designed so as to have a one-to-one mass ratio between the actuators and other parts. Based on the hydraulic servo actuator dynamics, the paper describes the details of velocity and force control of the robot joints, along to our passivity-based force control framework. Details on the hardware including the mechanisms, microcontrollers, and simulators are also described. Finally, the paper provides experimental results on zero-force tracking control, gravity compensation, task-space impedance control, and jumping.

I. INTRODUCTION

Recently, interest in agile legged locomotion technology has greatly increased [1], aiming at:

- 1) High robustness against strong disturbance
- 2) High locomotion speed

We also have been studying agile legged locomotion by creating the necessary research platform by ourselves. The platform is expected to have high-speed, compliance, and robustness so that we, users, can program and perform experiments very easily and quickly. The authors think hydraulic actuators are the best solution for this purpose. Actually, from the past studies on animal like fast running [2] to recent compliant full-body humanoid balancing control [6], the hydraulic robots used have never been broken. One-legged running robot *Kenken* [2], installed with bi-articular springs, is still working as a student tool in the author's laboratory. No mechanical part including the servo actuators were replaced at all. Hydraulic actuators are used mainly in aerospace industry, and not widely studied in robotics academy, although recently there have been great progresses in *hydraulic hybrid technology*. A recent activity on agile hydraulic robots is still limited to some research group supported by US military. However, the experience convinced us that hydraulic robots are useful for research platform or educational tool for robotics in general.

Another advantage of hydraulic actuators for legged robots is its force controllability. Force control was not common in legged robot literatures for long time except for few papers [4]. The authors invented a general passivity-based full-body force control framework, and first achieved gravity compensation and compliant balancing control using

All the authors are with Humanoid Systems Laboratory, Ritsumeikan University (Noji-Higashi 1-1-1, Kusatsu, Shiga 525-8577, Japan).
gen@fc.ritsumei.ac.jp

S. Hyon is also with ATR Computational Neuroscience Laboratories (Hikaridai 2-2-2, Souraku-gun, Kyoto 619-0288, Japan).

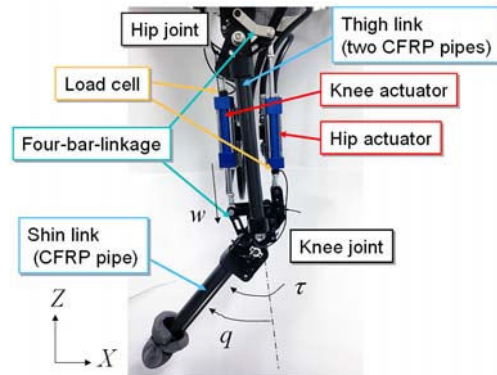


Fig. 1. Lightweight hydraulic leg testbed

SARCOS hydraulic humanoid robots [5][6][3]. The force controllability of the hydraulic actuator was the key points. Because of its compliance and natural behavior, currently many researchers are interested in force controlled humanoid robots.

Having obtained basic control technology, research interest is naturally shifted to the control software. Specifically, we need to make use of experimental data more effectively and intensively with some machine learning technique so that the robots acquire skillful motor control more quickly and robustly. Real-time optimal control is also becoming hot topics. However, this trend requires the robotic hardware to be tough and easy-use.

The purpose of the paper is to present our ongoing effort on building research platform suitable for exploring high-performance legged locomotion. First, this paper proposes to combine the hydraulic actuators with lightweight materials, for example, carbon-fiber-reinforced plastic (CFRP), so that we can maximally enjoy their high load-to-weight ratio. The more the robot is light and tough, the more the robot becomes agile. Also, the researcher's effort and the cost become small as well. Details on velocity and force controller and the experimental results are presented.

In the following, we describe the details of our first research platform: Lightweight hydraulic leg shown in Fig. 1. Section II reviews our passivity-based force control framework, and describes velocity and force control of hydraulic servo actuator, based on the actuator dynamics. Section III presents the details on the mechanism and controller of the robot. Section IV shows experimental results on high-speed swing control, zero-force tracking control, gravity compensation, virtual spring control, and jumping, to demonstrate the actual performance of the leg testbed.

II. FORCE AND TORQUE CONTROL WITH HYDRAULIC SERVO ACTUATOR

This section reviews our force controller with hydraulic servo actuator[11].

A. Task-space force control

Before explaining the hydraulic actuation, let us first briefly review a simple force control framework proposed in [5]. We introduce a *ground applied force* (GAF) $f_P = [f_{xP}, f_{yP}, f_{zP}]^T$, defined as $f_P := -f_R$, where f_R is the ground reaction force (GRF). The GAF represents the gross force that the robot applies to the environment. The control objective here is to bring f_P to the desired value \bar{f}_P , which is give by a task.

The simplest form of the passivity-based contact force control is given by

$$\tau = J_P^T \bar{f}_P - D\dot{q} \quad (1)$$

$$\bar{f}_P = f_u + Mg \quad (2)$$

where q is the generalized coordinate (joint angle), J_P is the Jacobian from the center of mass (CoM) to the *desired* center of pressure (CoP) and $f_u = [f_{ux}, f_{uy}, f_{uz}]^T$ is a certain new force input. This yields the convergence of GAF, $f_P \rightarrow f_u + Mg$ as $t \rightarrow \infty$, provided the joint-wise damping D (positive diagonal matrix) is designed so that the internal dynamics is stable as shown in the Appendix of [6]. See [7][8] and the related papers for passivity-based redundant manipulators.

For the extension of the above formula to multiple contact case, see [6], where the GAF is optimally distributed to multiple contact forces f_{Sj} ($j = 1, 2, \dots$), and the Jacobian J_P is replaced by the multi-contact Jacobian J_S . Any multi-legged robots including biped and quadruped robots can be handled in this simple and uniform framework [5]. It is also straightforward to include posture control or some desired joint motions. Important choice is whether to cancel dynamic effect or not, depending on how the dynamic model is precise.

B. Joint torque control by hydraulic actuators

The hydraulic cylinder combined with servovalve is *extremely stiff* actuator due to the high pressure gain [9]. This makes hydraulic servo actuators good velocity controlled actuators. This section provides technical details on force control using flow-controlled servo valves.

For simplicity, suppose the actuator is a double-rod cylinder driven by a servovalve as shown in Fig. 2. (We use different equations for single-rod cylinders, where the push area and the pull area are different.) The related variables are given in the figure. See Fig. 1 for the picture of the servo actuator installed in our robot.

We assume the valve dynamics from the input command to the output flow, which includes the current amplifier and the valve electro-magnetic system in Fig. 2, is fast enough. In this case, for a given pressure supply P_S and load pressure

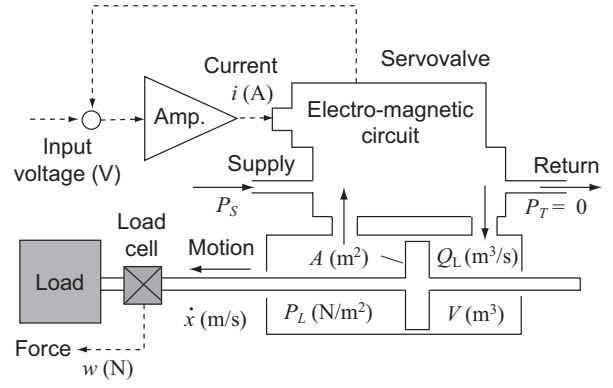


Fig. 2. Diagram of force feedback control by a hydraulic actuator with a flow-control servo valve. Notations: P_S : supply pressure, P_L : load pressure, P_T : return pressure, Q_L : load flow, A : piston area, V : cylinder chamber volume.

P_L (assuming the return pressure P_T is zero), the (static) load flow Q_L is given by

$$Q_L = K_i \sqrt{P_S - \text{sign}(i)P_L} \cdot i \quad (3)$$

where K_i is the current gain [10].

The velocity control is rather straightforward. Using $Q_L = A\dot{x}$, we simply invert (3) to obtain the input current from desired velocity \dot{x} :

$$i = \frac{1}{K_i \sqrt{P_S - \text{sign}(i)P_L}} \{i_{bias} + \dot{x}\} \quad (4)$$

where i_{bias} is defined below.

On the other hand, the load flow in the cylinder is given by

$$Q_L = A\dot{x} + C_{tp}P_L + \frac{V_0}{2\beta_e}\dot{P}_L \quad (5)$$

where β_e is the effective bulk modulus, C_{tp} is the total leakage coefficients, and V_0 is the initial volume of chamber. See [9] for details. Combined with some load dynamics (e.g. rigid body dynamics) and some cylinder friction model, one can simulate the total nonlinear dynamics. See [2] for the example on hydraulic one-legged hopping robot.

How about force control? One big advantage of hydraulic servo actuator is its high response. Thanks to this, we can employ force-sensor-feedback. This is simply done by using admittance controller, which transform the force error to the velocity command with some force feedback gain. Specifically, let us consider a simple force feedback controller. We apply (4) with

$$\dot{x} = -K_f(w - \bar{w}) \quad (6)$$

where K_f is the force feedback gain, $w = AP_L$ is the *measured* load, and \bar{w} is the desired load, which is commanded by the joint torque controller described in Section II-C. The valve bias is given by $i_{bias} = C_{tp}w/A$, which depends on the load.

Combining (3)–(6), the closed-loop dynamics becomes:

$$A\dot{x} + \frac{V_0}{2\beta_e}\dot{P}_L = -K_f(w - \bar{w}) \quad (7)$$

If the piston position is fixed ($\dot{x} = 0$), the load pressure P_L rapidly converges to $\bar{P}_L = \bar{w}/A$ because the coefficient $V_0/(2\beta_e)$ is very small. This corresponds to the so-called *fast dynamics* in standard singular perturbation methods [15]. By the same reason, we can disregard the dynamics of P_L from (7) to yield the approximated dynamics

$$A\dot{x} = -K_f(w - \bar{w}). \quad (8)$$

Therefore, we conclude that the actual force is given by

$$w = \bar{w} - \frac{A}{K_f}\dot{x}. \quad (9)$$

The second term plays an effective damping force in the actuator; if we connect the actuator with a simple load with mass m , the load dynamics becomes

$$m\ddot{x} = \bar{w} - \frac{A}{K_f}\dot{x}. \quad (10)$$

The larger force gain is, the smaller actuator damping is. In other words, we can change the damping D in (2) by simply tuning the force gains! A similar approach is applied also in recent hydraulic robots [12].

We may apply a simpler force feedback controller

$$i = -K_f(w - \bar{w}), \quad (11)$$

instead of (6), then we have both the steady state error and larger damping due to the uncompensated term. However, C_{tp} is in the order of 10^{-12} . Therefore, when $P_L = 0.5P_s$ for example, the equivalent force feedback gain reduces only by the factor of 0.71, with the small bias $0.5C_{tp}P_s$.

If the feedback is fast enough (faster than the mechanical resonance frequency) then we can control the force *as if* there were no sensory feedback. That is, the actuator behaves as an ideal force generator. The high-speed digital controller in Section III-D makes this possible (10 kHz local servo loop in our case).

C. Joint torque controller

If the joint, actuator and sensors are collocated, the implementation of a joint torque controller can be simplified as shown in (11). However, they are not collocated in our robot, as can be seen in Fig. 1. Therefore a joint torque controller is implemented on the on-board controller. The control module includes the joint-wise force-torque transformation based on the individual joint kinematics, together with the calibration factors.

The work flow of the torque controller is:

- (L1) Convert desired joint torques to the desired actuator forces;
- (L2) Calculate the reaction forces applied to the force sensors;
- (L3) Convert (L2) to the actuator reaction forces;
- (L4) Send (L1),(L3) and the force feedback gains to the low-level joint controllers.

Similar processing is used for the joint velocity controller as well.

TABLE I
JOINT SPECIFICATION

Joint	RoM deg	Max torque Nm	Max velocity deg/s
Hip flex./ext. (HFE)	-100 / 30	345	1370
Knee flex./ext. (KFE)	0 / 130	320	1490

III. HARDWARE OVERVIEW

Fig. 1 shows the leg testbed we fabricated. The leg has hip and knee joints, both actuated by a single rod hydraulic servo actuator. In this section we explain the details of the testbed.

A. Joint specification

The range of motion (RoM), maximum joint velocity and torque are determined based on some literatures on human running and measured data using motion capture system and force plates. Because of space limitations, we will skip the details on the human data. Table I shows the resultant joint specification of the robot with 21 MPa (3000 PSI) supply pressure. (For normal operation, 7 MPa is used.) Currently, the leg testbed with two-joints is 6 kg in weight, but we can reduce it to 4 kg without any compromise. The length of the link is 0.38 m.

B. Lightweight design with CFRP pipes and linear hydraulic actuators

Introduction of CFRP and hydraulic actuator for biped robot can be seen in Waseda WL-12 [13], one of the fast dynamic walking machines developed so far. However, in WL-12, rotary actuators have been used. Therefore, the actuators do not bear the structural load. In contrast, as can be seen from hydraulic excavator, the cylinder constitutes the member of the linkage. This reminds us truss structure, where only the tensile and compressive forces are applied to each member through the pivots. If the member is strong enough in longitudinal direction, we can make the robot lightweight, although care must be taken for buckling. CFRP best suits this purpose because strength can be easily specified at the manufacturing process. Hydraulic cylinders can generate large linear force, and strong in longitudinal direction (*at least*, up to the maximum actuator force).

This idea led us to the simple mechanism as shown in Fig. 1. To achieve lightweight, we aimed at *one-to-one mass ratio* between the actuator and the other parts. Two CFRP pipes are used for the thigh link, and the one for the shin link. FEM analysis is done for all the main parts using 3D CAD software (Solid Works). Four-bar-linkage mechanisms are introduced to ensure enough RoM inspired by SARCOS humanoid robot [14].

C. Hydraulic servo pump

Considering energy efficiency and power autonomy are of second importance in this study, but we tried to achieve efficiency as much as possible. The solution is introduction of the servo-controlled hydraulic pump. That is, servo motor

controls the supply pressure and flow very accurately and quickly. The pump is made by Daikin, and is used in some hydraulic hybrid excavators.

With this pump, basically, the controller commands low pressure when there is no need to generate high joint torques (or high speed), for example, when the robot is standing upright posture. Since servo valves at high pressure have a lot of leakage and cause heating, being at low pressure saves the electricity very much.

D. Digital controller

To achieve high-performance velocity and force control, we introduced a Microchip 16-bit dsPIC for MPU. Using the software libraries, 16-bit floating point arithmetic instruction is possible, which is powerful enough for low-level servo control for a single hybrid drive joint.

The controller has two servo amplifier. The joint angle is measured by an analog potentiometer. The controller has a differential amplifier to measure the strain of the force sensors. The controller has a 100-Mbps Ethernet interface, and communicates with the host PC with one cable. The communication speed between the controllers and PC depends on the communication software and buffer size. Currently, we have succeeded in stable real-time 500-Hz communication for all I/O signals for ten servo controllers.

The servo controller has a DSP (digital signal processor) specialized for fast multiplication/summation instruction. We utilize this for velocity and force control described in Section II, as well as conventional analog sensor filtering.

E. Simulator and controller interface

To concurrently conduct simulations and experiments, we developed an integrated control environment (ICE) using a dynamic simulator and a GUI, both of which are connected to the digital controller described in Section III-D. Fig. 3 shows two examples, where a biped humanoid robot and a quadruped robot, which we are actually building, are modeled. The GUI allows users to handle task-level (and even micro-controller-level) states (e.g., joint angles, torque, posture), input commands (e.g., desired angles, torque, CoM) either in the simulator or in the actual robots. Data logging and parameter setting are also supported. Dynamic or static properties of the actuators and sensors will be soon reflected so that we can monitor the state of the hardware easily.

IV. EXPERIMENT

This section presents the experimental performance of the robotic leg. The purpose is to show its speed and force tracking performance. The speed is almost determined by the cylinder and valve selection, while the force tracking performance is strongly limited by the valve, sensor, and controller bandwidth. Hence, the experimental evaluation is very important. Also, we are interested in how the performance changes according to the pressure supply.

As shown later in Fig. 7, the leg is attached to the plate, on which two hydraulic manifolds are attached. At the four corners of the plate is attached with linear bushes that enable

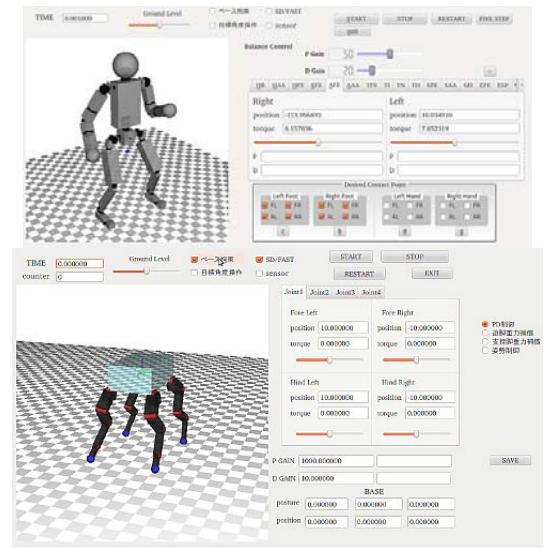


Fig. 3. Integrated controller interface for a biped humanoid robot and a quadruped robot: left window shows behaviors of either actual or simulated robots, or the right window is the control panel.

the plate move vertically along the four steel guides (180 mm in height) with extremely low friction. Safety springs are attached to the steel guides in case the robot foot slips the ground. The weight of the plate including the manifolds and linear bushes is 19 kg, hence the total weight is 25 kg. This is approximately the half of the expected weight of biped humanoid robots and a quadruped robots we are building.

The controller panel is put on the desk beside the robot. Hydraulic hoses from the hydraulic pump are connected to the two manifolds. An emergency switch enables the operator cut the hydraulic pressure. In addition, when the operator pushes keyboard, all the input currents to the servo valves are cut.

A. Zero-force tracking control

Fig. 4 shows the force tracking control performance where the commanded joint torque, hence the cylinder force, is set to zero. This emulates passive swinging of the leg. Recall that hydraulic actuators are extremely stiff in nature. Nevertheless, thanks to high-speed force feedback control, the leg behaves as if there were no actuators. Peak forces are intentionally applied by the operator to check the stability of the closed-loop systems against sudden huge disturbance. The pressure supply is set to 6 MPa.

B. Gravity compensation for swinging leg

Fig. 5 shows another force tracking control performance where the commanded joint torque is set to anti-gravitational torque, which is computed in host PC, not in digital servo controllers. Therefore, commanded cylinder force is sent at every 0.2 ms. The link parameters are identified by least square. The graph shows the non-zero torque control performance is good. The pressure supply is set to 6 MPa.

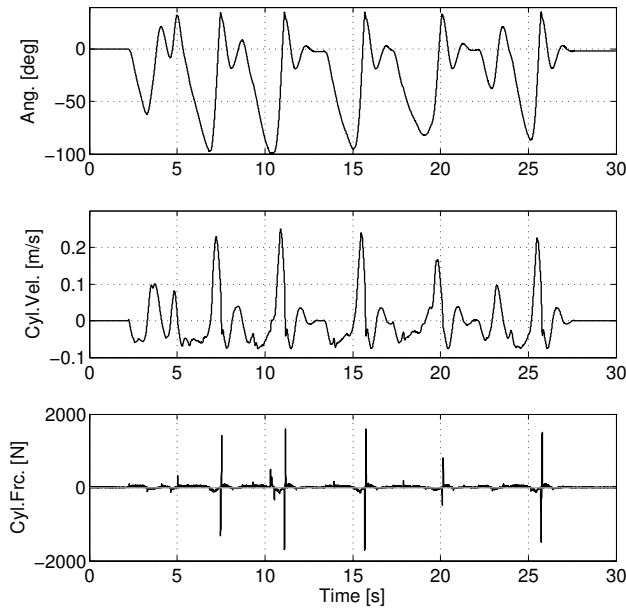


Fig. 4. Zero-force tracking experiment. Only the hip joint data is shown. The dark lines indicate actual values, and the light lines are the desired values. The large force peak shows the hip joint hits the limit. This is because the human operator is striking the link to the end to check the stability.

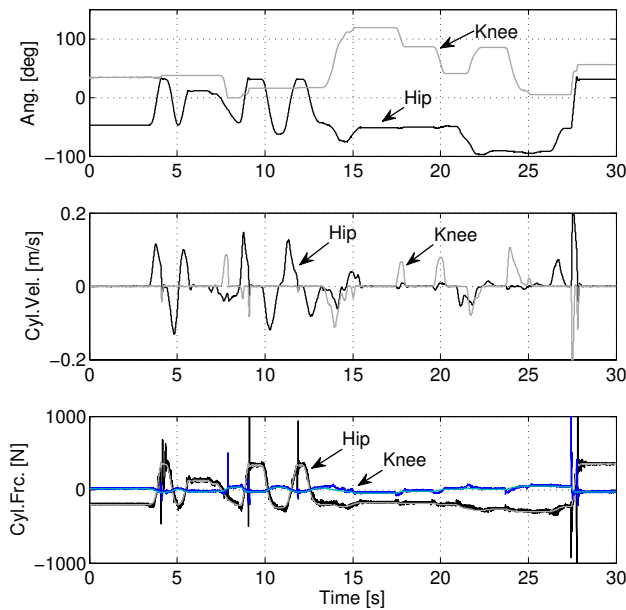


Fig. 5. Gravity compensation for swinging leg. The peak forces appear by the same reason as in Fig. 4.

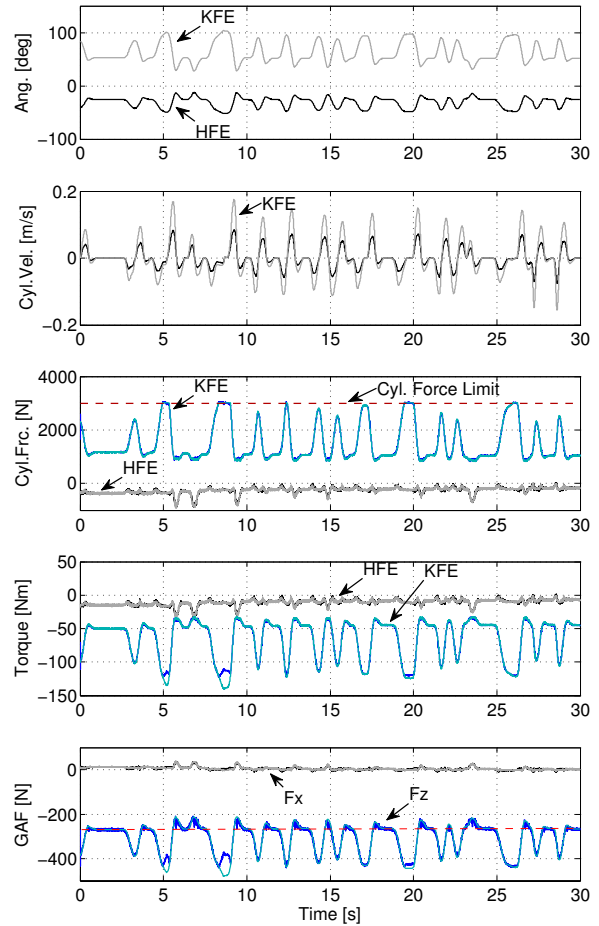


Fig. 6. Task-space impedance control (virtual spring control). The dashed line in the bottom figure indicate the anti-gravity force.

C. Impedance control

Gravity compensation at standing posture was also found to be good. The first 3 second time line of Fig. 6 shows the performance. This time, the supply pressure is set to 10 MPa.

From 3 second, the controller is moved on to impedance control mode. The equilibrium position of the foot is fixed to some initial position, and relatively low position feedback gain is set as the spring constant. The desired user force (2) is set to:

$$f_{ux} = -2000(x - x_d), \quad f_{uz} = -1000(z - z_d) \quad (12)$$

This allows the robot behave as if there is a spring between the plate and the ground. At every time a human operator applies external force, the robot is compliantly moves according to the target spring dynamics.

The bottom graph shows the ground reaction force calculated from the actual cylinder forces. Since the Jacobian matrix is regular, the calculated forces actually indicate the real GAF (negative GRF).

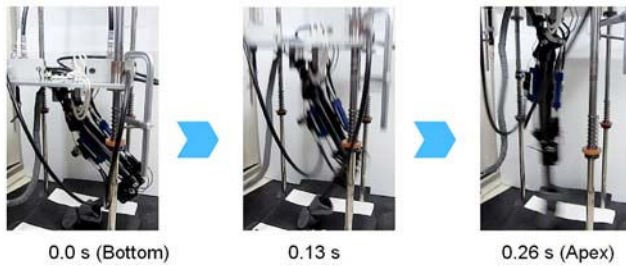


Fig. 7. Jumping experiment

D. Jumping and touchdown

Jumping is very fundamental motion for agile legged robots must perform easily. As a preliminary test, we tried to make the leg take off the ground by using a large vertical force f_{uz} . The take-off happens, when the knee joint angle becomes nearly extended. The desired horizontal force f_{ux} is fixed to zero so that the leg does not generate any resistive (horizontal) forces to the steel guides. Then, the controller switches to the same impedance control mode as above, where the desired position is set to a landing posture. Again, the supply pressure is set to 10 MPa.

Fig. 7 shows the snap shots of the jumping motion. Our robot can take off the ground, and compliantly interact with large external force such as impact forces. Although we use a soft mat on the floor, this can be considered as a shoe. Foot also can have compliance. This result is promising because we didn't apply any optimization (vertically-constrained motion is not optimal for high jump), the pressure is the half of the limit, and there is no ankle actuation.

Only the weak point is that the force control is based on strain gauge-type force sensors, which are fragile for large forces. This is why we set the maximum desired force to be 3000 N in this experiment (see the dashed line in the third graph). Some effective combination of the force sensors, pressure sensors, and various springs/dampers is left for future work.

V. CONCLUSION

The paper reported on a hydraulic robotic leg, a research platform suitable for exploring high-performance legged locomotion. We proposed to use hydraulic linear actuators combined with lightweight links made out from carbon-fiber-reinforced plastic so that we can maximally enjoy their innate high load-to-weight ratio. The robot was designed so as to have a one-to-one mass ratio between the actuators and other parts. Based on the hydraulic servo actuator dynamics, the paper described the details of velocity and force control of the robot joints, along to our passivity-based force control framework. Details on the hardware including the mechanisms, microcontrollers, and simulators were also described. This research platform was found to be quite useful for educational purpose. Actually, the robotic leg presented in this paper was designed and assembled by two undergraduate students within two years.

Finally, the paper provided experimental results on high-speed swing control, zero-force tracking control, gravity compensation, task-space impedance control, and jumping. The experimental graphs demonstrated that the proposed system is actually effective for research platform to explore agile legged locomotion, and possibly agile manipulation.

ACKNOWLEDGEMENT

We thank Ibaraki Industries for their support on the CFRP parts. We thank ASKK for their support on fabricating mechanical parts. We thank S. Ozaki for his support on digital controllers. We thank PSC for their support on hydraulic components. We thank Daikin for their support on hydraulic pumps. We thank Mizuno Tech. Inst. for their support on electrical systems. We thank T. Hosoyama and N. Oku for their support on experiments. We thank M. Otsuka and Dr. Isaka, College of Sport and Health Science, Ritsumeikan University, for providing motion data of sprinters. We thank ATR for their support on experimental facilities. We thank H. Mizui and Y. Mori for their support on hydraulic systems.

REFERENCES

- [1] DARPA Robotics Challenge web site. [Online]. <http://www.theroboticschallenge.org/>
- [2] S. Hyon, T. Emura and T. Mita, "Dynamics-based control of one-legged hopping robot," *Journal of Systems and Control Engineering*, Proceedings of the Institution of Mechanical Engineers Part I, vol.217, no.2, pp.83–98, 2003.
- [3] S. Hyon, J. Morimoto and M. Kawato, "From compliant balancing to dynamic walking on humanoid robot: Integration of CNS and CPG," *IEEE ICRA*, pp.1084-1085, 2010.
- [4] J. Pratt, C. Chew, A. Torres, P. Dilworth and G. Pratt, "Virtual model control: An intuitive approach for bipedal locomotion," *International Journal of Robotics Research*, vol.20, no.2, pp.129-143, 2001.
- [5] S. Hyon and G. Cheng, "Passivity-based full-body force control for humanoids and application to dynamic balancing and locomotion," in *IEEE/RSJ IROS*, 2006, pp. 4915–4922.
- [6] S. Hyon, J. G. Hale, and G. Cheng, "Full-body compliant human-humanoid interaction: Balancing in the presence of unknown external forces," *IEEE Trans. Robotics*, vol. 23, no. 5, pp. 884–898, 2007.
- [7] S. Arimoto, M. Sekimoto, H. Hashiguchi, and R. Ozawa, "Natural resolution of ill-posedness of inverse kinematics for redundant robots: a challenge to bernstein's degrees-of-freedom problem," *Advanced Robotics*, vol. 19, no. 4, pp. 401–434, 2005.
- [8] A. Albu-Schaffer, C. Ott, and G. Hirzinger, "A Unified Passivity-based Control Framework for Position, Torque and Impedance Control of Flexible Joint Robots," *The International Journal of Robotics Research*, vol. 26, no. 1, pp. 23–39, 2007.
- [9] H. Merrit, *Hydraulic Control Systems*, Wiley, 1967.
- [10] MOOG web site. [Online]. <http://www.servovalve.com>
- [11] S. Hyon, "A motor control strategy with virtual musculoskeletal systems for compliant anthropomorphic robots," *IEEE/ASME Transactions on Mechatronics*, vol. 14, issue 6, pp. 677–688, 2009.
- [12] T. Boaventura, C. Semini, J. Buchli, M. Frigerio, M. Focchi and D.G. Caldwell, "Dynamic torque control of a hydraulic quadruped robot," in *IEEE ICRA*, 2012.
- [13] J. Yamaguchi, N. Kinoshita, A. Takanishi, and I. Kato, "Development of a dynamic biped walking system for humanoid development of a biped walking robot adapting to the humans' living floor," in *IEEE International Conference on Robotics and Automation*, vol. 1, 1996, pp. 232–239.
- [14] G. Cheng, S. Hyon, J. Morimoto, A. Ude, J. G. Hale, G. Colvin, W. Scroggin, and S. C. Jacobsen, "CB: A humanoid research platform for exploring neuroscience," *Advanced Robotics*, vol. 21, no. 10, pp. 1097–1114, 2007.
- [15] H. K. Khalil, *Nonlinear Systems*, 2nd ed, Prentice Hall, 1996.